INTERNATIONAL JOURNAL FOR NUMERICAL METHODS IN FLUIDS, VOL. 18, 843–852 (1994)

A MULTIGRID METHOD FOR PREDICTING PERIODICALLY FULLY DEVELOPED FLOW

L. BAI, N. K. MITRA, M. FIEBIG AND A. KOST

Institut für Thermo- und Fluiddynamik, Ruhr-Universität Bochum, Postfach 102148, W-44780 Bochum 1, Germany

SUMMARY

The use of multigrid methods in complex fluid flow problems is still under development. In this paper a full multigrid procedure has been incorporated in a finite volume solution for predicting fully developed fluid flow in a streamwise periodic geometry. Steady computations in two-dimensional body-fitted co-ordinates have shown considerable savings in computation time by this multigrid method.

KEY WORDS Multigrid Periodicity Body-fitted co-ordinates

1. INTRODUCTION

Fluid flow and heat transfer in streamwise periodic geometries such as channels with built-in bundles of tubes, grooved channels or ribbed channels are extensively used in industry. Their corresponding study is an area of increasing importance in both experimental and numerical contexts.

The workload for numerical prediction of the flow field and heat transfer in such a geometry can be tremendously reduced if the flow is modelled to be periodically fully developed. This allows the flow field to be decomposed into elements with identical (often in some non-dimensional sense) flow structure. One can choose one element with periodic boundary conditions as the computational domain for the flow simulation. However, because of the inherent iterative nature of the computational scheme caused by the unknown inlet or exit condition, the computations may become prohibitively time-consuming, especially for solutions with fine grids.

The multigrid method is an iterative procedure which ideally exhibits a grid-independent convergence rate. The potential of this method has been demonstrated in the solution of various problems, both linear and non-linear.[1] However, to our knowledge, the multigrid method has not yet been applied to periodic flow problems.

The aim of this paper is to design and test a multigrid procedure for a periodic flow problem. The flow is described by the full Navier–Stokes equations.

We describe a full approximation scheme–full multigrid (FAS–FMG) cycling algorithm applied to a finite volume discretization on a collocated grid. The special treatment for the periodicity condition is also given. The SIMPLEC[2] pressure correction scheme is used as smoother for the Navier–Stokes equations. Finally, results for fully developed fluid flow over periodically ordered cyclindrical obstables placed between two parallel plates (Figure 1) are presented to demonstrate the effect of the multigrid method.

CCC 0271–2091/94/090843–10

Received March 1993
Revised December 1993

2. MATHEMATICAL MODEL

2.1. Basic equations

Figure 1 shows the schematic diagram of a two-dimensional channel with periodically built-in cylindrical obstacles. This geometry can be seen as an idealization of the plate–tube heat exchanger. Since the flow is assumed to be periodically fully developed, computation in only one element, shown by the dashed line in Figure 1, is sufficient to present the flow field.

Furthermore, because of the steady state situation, we can use only symmetrical half-region for calculation (Figure 2). For the purpose of applying the periodic boundary conditions, the computational region 'acfh' is extended by a small region 'cdef' (Figure 2). The actual solution domain is thus 'adeh.'.[3]

The Navier–Stokes equations for steady, two-dimensional, incompressible, laminar flow in body-fitted co-ordinates using Cartesian velocity components are written in the following form:

u_1-component

$$\sum_{i=1,2} \frac{\partial}{\partial x_i}\left[U_i u_1 - \frac{\mu}{J}\left(\sum_j B_j^i \frac{\partial u_1}{\partial x_j} + \sum_j \beta_j^i \omega_1^j\right) + p\beta_1^j\right] = 0, \tag{1}$$

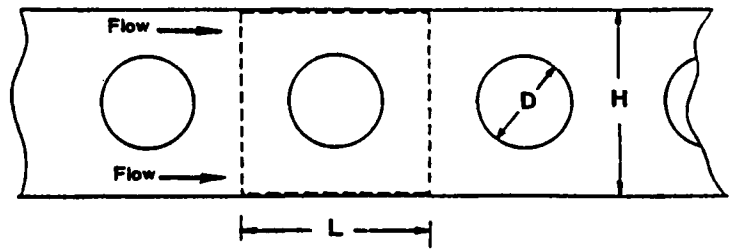

Figure 1. Schematic of the plate-bube arrangement.

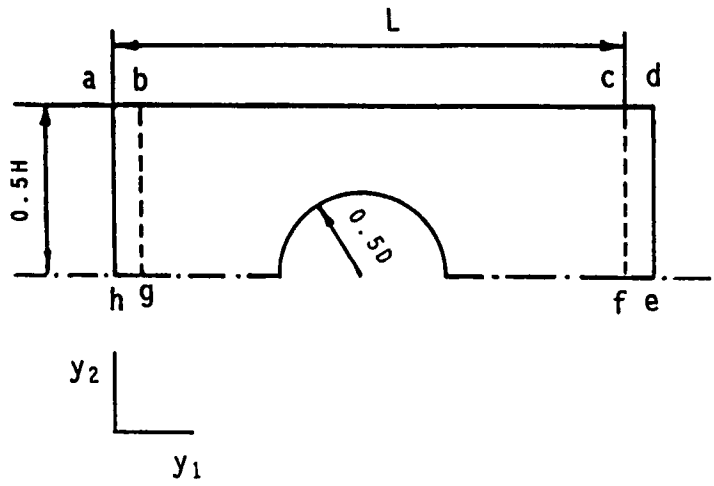

Figure 2. Schematic of the solution domain.

u_2-component

$$\sum_{i=1,2} \frac{\partial}{\partial x_i}\left[U_i u_2 - \frac{\mu}{J}\left(\sum_j B_j^i \frac{\partial u_2}{\partial x_j} + \sum_j \beta_j^i \omega_2^j\right) + p\beta_2^i\right] = 0, \tag{2}$$

continuity equation

$$\sum_{i=1,2} \frac{\partial U_i}{\partial x_i} = 0, \tag{3}$$

where

$$U_i = \rho \sum_j u_j \beta_j^i, \qquad B_j^i = \sum_k \beta_k^i \beta_k^j, \qquad \omega_j^i = \sum_k \frac{\partial u_i}{\partial x_k} \beta_j^k.$$

2.2. Boundary conditions

The following boundary conditions for one module are used. No-slip conditions on the top wall and the tube wall give

$$u_1 = u_2 = 0.$$

On the symmetry line the gradients of the velocities are set equal to zero:

$$\nabla u_1 = \nabla u_2 = 0.$$

Periodic conditions at the inlet and outlet give

$$u_1(0, y_2) = u_1(L, y_2), \qquad u_2(0, y_2) = u_2(L, y_2).$$

3. NUMERICAL METHODS AND COMPUTATIONAL DETAILS

The basic equations are solved by a SIMPLEC-based finite volume technique on collocated grids in body-fitted co-ordinates.

3.1. Discretization

The equations are discretized by employing a finite volume approach. The flow domain is subdivided into a finite number of continuous control volumes (CVs). The computational nodes are placed at the centre of each CV. All the dependent variables are defined at the centre point P. Figure 3 shows a typical control volume with labels.

Since the main emphasis here is on the effectiveness of the multigrid method rather than on the accuracy of the solution, upwind differences for convection terms are used. The viscous terms are discretized by central differences. The resulting finite volume discretization for the momentum equations can be written as

$$A_P \phi_P = \sum_{nb} A_{nb} \phi_{nb} + Sc\Delta V, \qquad A_P = \sum_{nb} A_{nb} - Sp\Delta V, \tag{4}$$

where nb = E, W, N, S, or in matrix form as

$$\mathbf{A\Phi} = \mathbf{S}. \tag{5}$$

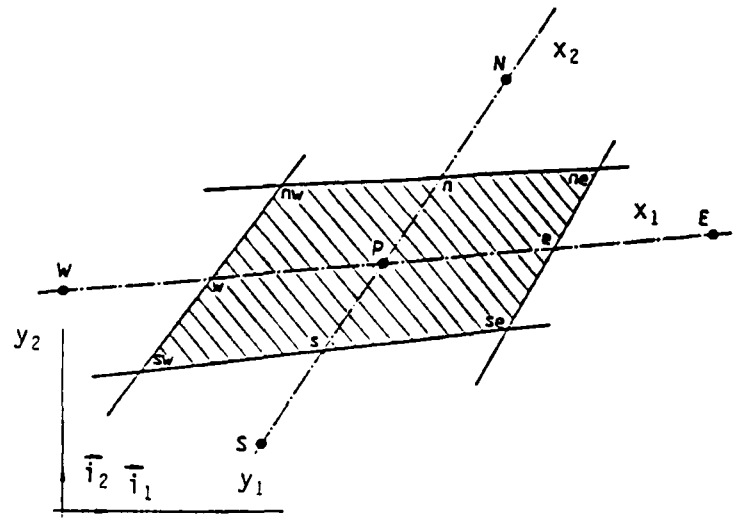

Figure 3. Two-dimensional control volume and the labelling scheme.

The coefficients A_{nb} contain the combined effect of convection and diffusion. Their detailed expressions can be found in Reference 4.

3.2. Pressure correction method

The velocity and pressure fields are interactively calculated with the SIMPLEC algorithm. In the collocated grid the velocities at the CV faces are to be calculated from the adjacent CV-centred quantities. In order to avoid oscillation, a special interpolation[4] is employed.

The CV-centred velocity u_P from the discretized u_1-momentum equation using the relaxation factor α_u is

$$u_P = \alpha_u\left(\frac{\sum A_{nb}u_{nb} + Sc\Delta V}{A_P} + D_1^1(P_e - P_w) + D_2^1(P_n - P_s)\right) + (1 - \alpha_u)u_P^o, \tag{6}$$

where

$$D_j^1 = -b_j^1/A_P. \tag{7}$$

Here the pressure difference terms have been taken out of the term $Sc\Delta V$. The relation for velocity is necessary.

Similar to the basic concept of staggering, the interpolations for the velocities at the CV faces, e.g. at the 'e'-faces, are given by

$$u_e = \alpha_u\left(\overline{\frac{\sum A_{nb}u_{nb} + Sc\Delta V}{A_P}} + \frac{1 - \alpha_u}{\alpha_u}u_P^o + D_1^2(P_n - P_s) + \overline{D_1^1}(P_E - P_P)\right). \tag{8}$$

The overbars represent the linear interpolations to the 'e'-faces. According to the SIMPLEC algorithm, the velocity corrections at the CV 'e'-faces are related to the pressure corrections as follows:

$$U_e' = \overline{\left(-\frac{b_1^1}{A_P/\alpha_u - \sum_{nb} A_{nb}}\right)}(P_E' - P_P'). \tag{9}$$

The formulae for the u_2-component are similar. The details of these derivations can be found in Reference 4. The continuity equation in discrete form gives

$$F_e + F_w + F_n + F_s = 0. \tag{10}$$

With

$$F_e = F_e^* + F_e'$$

and

$$F_e^* + F_w^* + F_n^* + F_s^* = S_m,$$

one obtains

$$F_e' + F_w' + F_n' + F_s' = -S_m. \tag{11}$$

From these equations we get the pressure correction equation, which is expressed in the form

$$A_P \phi_P = \sum_{np} A_{nb} \phi_{nb} + S_m, \qquad A_P = \sum_{nb} A_{nb}, \tag{12}$$

where nb = E, W, N, S.

The strongly implicit procedure (SIP) of Stone[5] is used here to solve the equations for u_1, u_2 and the pressure correction. Within each SIMPLEC procedure only one iteration is performed for the momentum equations (4), while the pressure correction equation (12) is iterated until the residual norm is reduced by a factor of $\frac{1}{4}$ or a maximum of 10 iterations is reached.

When all three normalized residual norms are reduced below 10^{-3}, convergence is assumed.

3.3. Implementation of periodic velocity boundary condition

As mentioned before, in the present study the solution domain is larger than one module by a small region. For the coarsest grid two volumes in the direction of the main flow are included in this region, while for a fine grid the number of volumes equals 2^n, where superscript n denotes the level of the grids. To start the iteration, a uniform velocity is assumed. The velocities at the inflow and outflow boundaries are treated as known. After one cycle of iteration, which includes a SIMPLEC procedure as defined before for the single-grid method and as defined in Section 3.5 for the multigrid method, the periodic boundary conditions are imposed by replacing the velocities on line 'ah' with the computed values on 'cf' and by replacing the velocities on line 'de' with the computed values on line 'bg'. This procedure is repeated until periodicity is attained. The details for the multigrid method are given in Section 3.5. To satisfy the mass balance, after each replacement the velocities at the inlet boundary and outlet boundary are redetermined by multiplying them respectively by a factor which is the ratio of the desired average velocity to the current average one.

3.4. Grid generation

The differential grid generation method[6] is used. This method, which allows us to control angles and distances of grid lines near a boundary, is applied to determine the source terms in the Poisson equations.[7]

The multigrid procedure first generates the finest grid. Four fine grid CVs are joined into one coarser grid CV, which is then defined by the four vertices of the fine grids. Figure 4 shows the four grids of the test problem.

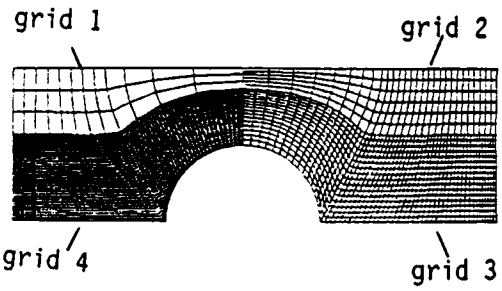

Figure 4. Four-level grids represented in one picute.

3.5. Multigrid method

The full approximation scheme (FAS)[1] is adopted in this paper. By applying several smoothing sweeps with the SIMPLEC algorithm on the fine grid, from equation (5) we obtain

$$\mathbf{S} - \mathbf{A}\boldsymbol{\Phi} = \mathbf{R}. \tag{13}$$

For the exact solution the residuum $\mathbf{R}$ reduces to zero, i.e.

$$\hat{\mathbf{S}} - \mathbf{A}\hat{\boldsymbol{\Phi}} = 0. \tag{14}$$

Subtracting equation (13) from equation (14) and transferring this equation to the coarse grid H, the FAS coarse grid equation becomes

$$\mathbf{A}^{\mathrm{H}}\hat{\boldsymbol{\Phi}}^{\mathrm{H}} = \hat{\mathbf{S}}^{\mathrm{H}} - I_{\mathrm{h}}^{\mathrm{H}}\tilde{\mathbf{S}}^{\mathrm{h}} + \mathbf{A}^{\mathrm{H}}I_{\mathrm{h}}^{\mathrm{H}}\tilde{\boldsymbol{\Phi}}^{\mathrm{h}} + I_{\mathrm{h}}^{\mathrm{H}}\tilde{\mathbf{R}}^{\mathrm{h}}, \tag{15}$$

where $I_{\mathrm{H}}^{\mathrm{h}}$ need not be the same for different variables. The 'tilde' on variables represents the current approximate solution on the finer grid h, while the 'hat' variables denotes the variables which are being modified in the course of iteration on the coarser grid H.

The approximate coarse grid correction is of course $\hat{\boldsymbol{\Phi}}^{\mathrm{H}} - I_{\mathrm{h}}^{\mathrm{H}}\tilde{\boldsymbol{\Phi}}^{\mathrm{h}}$, so the FAS interpolation back to the fine grid is

$$\boldsymbol{\Phi}_{\mathrm{new}}^{\mathrm{h}} = \boldsymbol{\Phi}_{\mathrm{old}}^{\mathrm{h}} + I_{\mathrm{H}}^{\mathrm{h}}(\hat{\boldsymbol{\Phi}}^{\mathrm{H}} - I_{\mathrm{h}}^{\mathrm{H}}\tilde{\boldsymbol{\Phi}}^{\mathrm{h}}), \tag{16}$$

where $I_{\mathrm{H}}^{\mathrm{h}}$ and $I_{\mathrm{h}}^{\mathrm{H}}$ denote bilinear interpolation for prolongation and restriction respectively.

Since a collocated grid is imployed, the residuals of the coarse grids can be restricted by summing the residuals of the four related fine grid CVs. For consistency reasons the source term $I_{\mathrm{h}}^{\mathrm{H}}\tilde{\mathbf{S}}^{\mathrm{h}}$ is determined by the restricted $I_{\mathrm{h}}^{\mathrm{H}}\tilde{\boldsymbol{\Phi}}^{\mathrm{h}}$, so that when $\tilde{\mathbf{R}}^{\mathrm{h}}$ equals zero, the coarse grid equation (15) becomes an identity.[8]

For the linear pressure operator only the correction on the coarse grid is necessary for the fine grid pressure. The correction is obtained through the pressure correction equation.

The full multigrid (FMG) algorithm is employed. Figure 5 shows the FMG cycle applied to periodic flow. The numbers in circles indicate the iteration sweeps which are performed on each grid level. The numbers in squares denote the grid levels where an accurate solution will be attained. On the finest grid two iteration sweeps are first performed, followed by two iteration sweeps for smoothing. After each of the smoothing iterations the maximum absolute difference between the velocities on lines 'cf' and 'ah' and between the velocities on lines 'bg' and 'de' (Figure 2) is computed. If this maximum is not smaller than a desired value (0·5% of the mean velocity in this study), the periodic boundary conditions are imposed by replacing the corresponding velocities as explained before. Otherwise the replacement is not performed.

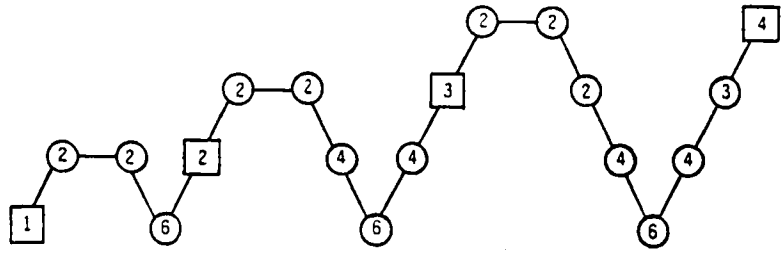

Figure 5. Full Multigrid scheme.

4. RESULTS AND DISCUSSION

For the test problem the geometry parameters are taken as $H/D = 2$ and $L/D = 3$. The computations are done for $Re = 50$ and 100. When the Reynolds number is not larger than 100, the flow remains steady.[9] It is therefore reasonable to choose the half-region as solution domain (Figure 2).

The streamlines and velocity vectors predicted on the finest grid for the flow state at $Re = 100$ are presented in Figure 6.

From these pictures we can see that the periodicity of the flow is well realized.

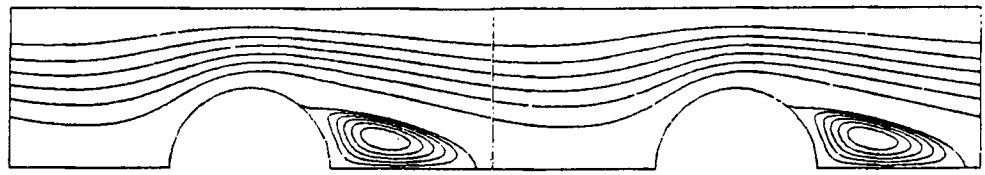

(a)

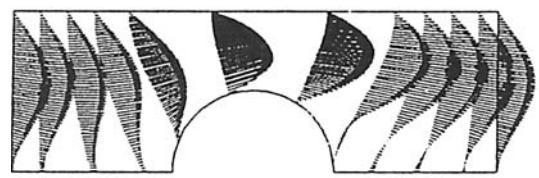

(b)

Figure 6. (a) Computed streamlines, (b) velocity vectors; H/D = 2, L/D = 3, Re = 100.

Table I. Computation times and iteration numbers for single-grid (SG) and multigrid (MG) schemes

	Computation time (CPU seconds)				Number of iterations			
CVs	26 × 7	52 × 14	104 × 28	208 × 56	26 × 7	52 × 14	104 × 28	208 × 56
				Re = 50, $\alpha_u = 0{\cdot}8(0{\cdot}9$ *for SG)*				
SG		7·43	90·97	1508·64		45	130	450
MG	1·32	5·57	36·71	187·71	40	29	39	39
MG/SG		72%	40%	12%				
				Re = 100, $\alpha_n = 0{\cdot}8(0{\cdot}9$ *for SG)*				
SG		8·67	84·77	1368·73		57	128	423
MG	1·47	8·52	58·04	260·92	45	51	55	51
MG/SG		98%	68%	19%				

Table I lists the computation times and iteration numbers for the multigrid and single-grid methods. For the multigrid method the iteration number is that performed on the finest grid. A comparison of the computation times between single-grid and multigrid methods is also given in Table I. The calculations were performed on a Cyber 992 computer.

For the coarser grids the savings by multigrid are not large, and with an increase in grid number (from grid 1 to grid 2, from grid 2 to grid 3) the increase in the computation time is faster than linear, i.e. the grid-independent convergence rate has not been attained. One of the reasons for this is the influence of the extra iterations resulting from the periodic conditions. For the finer grids the behavior of the multigid method has been well demonstrated. From grid 3 to grid 4 the convergence rate of multigrid is almost independent of the number of control volumes, and the computation time increases approximately linearly. In contrast, the computation time of single-grid increases quadratically, i.e. the influence of the periodic conditions on the calculation feature becomes small. For finest grid of this study (208 × 56 DVs) the savings in computation time by the multigrid method are 88% and 81% for $Re = 50$ and 100 respectively. The saving in computation time will increase if an even finer grid is adopted. One notices that the relative efficiency of the multigrid method decreases as the Reynolds number increases. One reason for this is that with increasing Reynolds number the effect of the SIMPLE-type method as smoother for the multigrid method decreases.[10] Another reason for the smaller saving at high Reynolds number is that the base method converge increasingly faster.

5. CONCLUSIONS

The FAS–FMG method has been successfully applied to predict periodically fully developed flow. Computations for two-dimensional, steady, incompressible fluid flow in body-fitted co-ordinates have shown that approximately grid-independent convergence can be attained with a fine grid, and that considerable savings in computation time can be achieved by the multigrid method.

ACKNOWLEDGEMENT

This work has been supported by the Deutsche Forschungsgemeinschaft (SFB 278), for which the authros wish to express their gratitude.

APPENDIX: NOMENCLATURE

A	coefficients of fine volume equation
$\mathbf{A}$	matrix form of coefficients
b_j^i	projection area of control volume
D	cyclinder diameter
D_j^i	pressure coefficient (equation (7))
F	mass flow
H	width of channel
I_h^H	some fine-to-coarse transfer, defined in text
I_H^h	bilinear interpolation from coarse grid to fine grid
J	Jacobian of co-ordinate transformation $y_i = y(x_i)$
p	pressure
S	source term, $S = Sc + Sp\phi_P$
$\mathbf{S}$	matrix form of source term
Sc	constant part of linearized source terms
Sp	coefficient of ϕ_P in linearized source term
S_m	mass imbalance (equation (11))
$\mathbf{R}$	residuum in matrix form
Re	Reynolds number, $Re = \rho u_m H/\mu$
u_m	average velocity
u_1, u_2	velocity components in y_1- and y_2-directions
x_1, x_2	arbitrary co-ordinates
y_1, y_2	Cartesian co-ordinates

Greek letters

α_u	underrelaxation factor for velocity components u_1 and u_2
β_j^i	cofactor of $\partial y/\partial x$ in J
ΔV	control volume
μ	dynamic viscosity
ρ	density
ϕ	variable representing u_1, u_2 or p'
Φ	matrix form of arbitrary variable

Superscripts

h	fine grid
H	coarse grid
i, j, k	convariant component of a vector or tensor
o	value of last iteration
*	uncorrected value
'	correction

Subscripts

e, n, s, w	control faces (Figure 2)

E, N, P, S, W	grid points (Figure 2)
h	fine grid
H	coarse grid
i, j, k	convariant component of a vector or tensor
nb	neighbouring grid points
ne, nw, se, sw	values associated with control volume vertices

REFERENCES

1. A. Brandt, *Multigrid Techniques: 1984 Guide with Applications to Fluid Dynamics, GMD-Studien No. 85*, GMD, Bonn, 1984.
2. J. P. Van Doormal and G. D. Raithby, 'Enhancements of the SIMPLE method for predicting incompressible fluid flow', *Numer. Heat Transfer*, **7**, 147–163 (1984).
3. R. C. Xin and W. Q. Tao, 'Numerical prediction of laminar flow and heat transfer in wavy channels of uniform cross-sectional area', *Numer. Heat Transfer*, **14**, 465–481 (1988).
4. M. Peric, 'A finite volume method for the prediction of three-dimensional fluid flow in complex ducts', *Ph.D. Thesis*, University of London, 1985.
5. H. L. Stone, 'Iterative solution of implicit approximations of multi-dimensional partial differential equations', *SIAMJ. Numer. Anal.*, **5**, 530–548 (1968).
6. J. F. Thompson, Z. U. A. Warsi and C. W. Mastin, *Numerical Grid Generation, Foundation and Application*, 1st edn., North-Holland, Amsterdam, 1985, Chap. 6.
7. A. Hilgenstock, 'A fast method for the elliptic generation of three-dimensional grids with full boundary control', in S. Sengupta, J. Häuser, P. R. Eiseman and J. F. Thompson (eds.), *Numerical Grid Generation in Computational Fluid Mechanics '88*, Pineridge, Swansea, 1988, pp. 137–146.
8. M. Hortmann and M. Peric, 'Finte volume multigrid prediction of laminar natural convection: bench-mark solution', *Int. j. numer. methods fluids*, **11**, 187–207 (1990).
9. D. Kunda, A. Haji-Sheikh and D. Y. S. Lou, 'Pressure and heat transfer in cross flow over cylinders between two parallel plates', *Numer. Heat Transfer*, **19**, 345–360 (1991).
10. G. J. Show and S. Sivaloganthan, 'On the smoothing properties of SIMPLE pressure-correction algorithm, *Int. j. numer. methods fluids*, **8**, 441–461 (1988).